Multiple-Pulse Nuclear-Magnetic-Resonance Transients of Xe^{129} and Xe^{131} in Solid Xenon*†

WILLIAM W. WARREN, JR.,‡ AND R. E. NORBERG
Department of Physics, Washington University, Saint Louis, Missouri
(Received 18 July 1966)

Transient nuclear free-precession signals have been investigated for Xe^{129} and Xe^{131} in solid xenon. Coherent radiofrequency pulses with controlled phase differences were used to produce "solid" echoes and "quadrupole" echoes which provide information about static dipolar and quadrupolar interactions in the solid. "Conventional" Xe^{131} echoes formed by rephasing in the external magnetic-field inhomogeneity were observed at temperatures for which the central transition of the Xe^{131} spectrum is motionally narrowed by self-diffusion. The temperature dependence of the data is consistent with the correlation times for self-diffusion obtained in previous Xe^{129} experiments.

I. INTRODUCTION

THE time dependence of the nuclear free induction decay which occurs after application of a 90° pulse at the nuclear Larmor frequency contains useful information about spin-dependent interactions of nuclei in solids.[1] Unfortunately, in cases where several types of interaction are present, analysis of the free-induction decay is complicated by the problem of separating the effects of the various interactions. Moreover, important portions of the nuclear signal often occur during the "dead time" or "blocking time" of the pulsed nuclear-magnetic-resonance apparatus. For the study of magnetic dipole-dipole and static electric quadrupole interactions, these problems may be overcome to some extent by the use of appropriate multiple-pulse sequences.[2–5] These sequences produce free precession signals known as "solid" or quadrupole echoes according to whether they are produced by dipolar or quadrupolar interactions, respectively. Such echoes are distinct from "conventional" spin echoes[6,7] in that their formation does not depend on an inhomogeneity in the applied external field. This paper describes observations of multiple pulse transients for Xe^{129} and Xe^{131} in solid natural xenon at 4.2°K, and conventional spin echoes for Xe^{131} at temperatures at which the resonance line is motionally narrowed by self-diffusion.

The theory of multiple pulse transients in rigid dipolar-broadened systems has been developed for a number of pulse sequences by Mansfield.[4] These calculations show, for example, that in a system containing a single magnetic species, the effect of a sequence of two 90° pulses differing in phase by 90° and separated by a time τ (90°-τ-90°$_{90°}$ sequence) is formation of a "solid" echo at $t=2\tau$ where $t=0$ is the time of the initial 90° pulse. The analysis shows that if τ is sufficiently small compared to the duration of the free-induction decay, the solid echo shape accurately reproduces the free-induction-decay shape. This permits analysis of the decay shape in the region that is normally masked by the blocking time of the pulsed spectrometer.

In a system containing two magnetic species I and S, the theory indicates that a well-defined solid echo may be observed following a 90°-τ-90°$_{90°}$ sequence if σ_{II}^2, the contribution to the second moment arising from interactions among the resonant species, is large compared with the contribution σ_{IS}^2 of interactions between the resonant species I and the nonresonant species S. On the other hand, if $\sigma_{IS}^2 \gg \sigma_{II}^2$, the theory predicts that a solid echo will not occur. Further, Mansfield has shown that application of a pair of "in-phase" 90° pulses (90°-τ-90°$_{0°}$ sequence) to a system containing two species should result in formation of an echo-like signal whose initial slope is a function of σ_{IS}^2 and τ. He has described a procedure for measuring σ_{IS}^2 directly by analyzing the dependence of this signal on the pulse spacing τ. A third sequence which is of interest for a system containing two species is a 90°-τ-180°$_{0° \text{ or } 90°}$ sequence. It is easy to show[8] that for sufficiently short τ, the height of the echo occuring at $t=2\tau$ approaches the magnitude that the free-induction decay would have at $t=2\tau$ if the nonresonant species were not present. There exists, therefore, the possibility of measuring the resonant spin contribution σ_{II}^2 with this type of solid echo.

In solids which nominally exhibit cubic symmetry, crystalline defects usually introduce random distributions of electric field gradients.[9] In such solids, the resonance lines of nuclei possessing electric quadrupole moments are broadened, often to such an extent that only the central ($m=\pm\frac{1}{2}$) transition can be seen by conventional steady-state techniques. If the root-mean-

* Based on a thesis submitted by William W. Warren, Jr. in partial fulfillment of the requirements for the degree of Doctor of Philosophy in The Graduate School of Arts and Sciences, Washington University.

† Supported by the U. S. Army Research Office (Durham) and an equipment-loan contract from the Office of Naval Research.

‡ National Science Foundation Cooperative Graduate Fellow, 1962–65. Present address: Department of Physics, University of California, Los Angeles, California.

[1] I. J. Lowe and R. E. Norberg, Phys. Rev. **107**, 46 (1957).
[2] I. Solomon, Phys. Rev. **110**, 61 (1958).
[3] J. G. Powles and J. H. Strange, Proc. Phys. Soc. (London) **82**, 6 (1963).
[4] P. Mansfield, Phys. Rev. **137**, A961 (1965).
[5] J. Butterworth, Proc. Phys. Soc. (London) **86**, 297 (1965).
[6] E. L. Hahn, Phys. Rev. **80**, 580 (1950).
[7] H. Y. Carr and E. M. Purcell, Phys. Rev. **94**, 630 (1954).
[8] W. W. Warren, thesis, Washington University, 1965 (unpublished).
[9] G. D. Watkins and R. V. Pound, Phys. Rev. **89**, 658 (1953).

square quadrupolar interaction is much larger than the dipolar spin-spin interaction, the result of such quadrupolar broadening in a pulsed NMR experiment is production of a two-component free-induction decay. In the limit of very large radiofrequency field H_1 and very short blocking time, one sees a rapidly decaying initial transient (corresponding to the quadrupolar broadened satellite lines) followed by a much longer "dipolar" decay whose shape is related to the shape of the dipolar broadened central transition.

Solomon[2] has applied the density-matrix formalism to calculate the transient response of a system of nuclei experiencing first-order quadrupolar interactions in an imperfect cubic crystal. If dipolar interactions are neglected, the calculation shows that the amplitude of the free-precession signal for $I=\frac{3}{2}$ is

$$S(t)=S(0)\left[\frac{3}{5}\int_{-\infty}^{\infty} f(a)\cos(2at)da+\frac{2}{5}\right], \quad (1)$$

where $a=3eQV_{zz}/4I(2I-1)\hbar$, Q is the nuclear quadrupole moment, and V_{zz} is the electric field gradient in the direction of the magnetic field. The function $f(a)$ describes the distribution of electric field gradients in the solid. The weaker dipolar interactions cause the "time-independent" component of Eq. (1), namely $\frac{2}{5}S(0)$, to decay in a characteristic time T_2.

In principle, one could study the gradient distribution $f(a)$ by analyzing the initial portion of the free-induction decay. This may be difficult in practice if the apparatus blocking time is of the same order as the duration of the quadrupolar free-induction decay. Solomon[2] has shown that application of a second pulse of rotation angle β at time $t=\tau$ will produce one or more quadrupole echoes whose shapes are given by the Fourier transforms of $f(a)$ and which may be used to observe the electric-field-gradient distribution. If the two pulses are in phase ($90°$-τ-$\beta_0°$ sequence), Solomon's theory shows that, for $I=\frac{3}{2}$, the height of the signal following the second pulse (relative to the magnitude of the free-induction decay immediately preceding the application of the second pulse) should be

$$S(t)=-(9/8)\sin^2\beta\cos\beta\int_{-\infty}^{\infty} f(a)[\cos 2a(t-2\tau)]da + (1/4)(\cos\beta)(9\cos^2\beta-5). \quad (2)$$

This sequence thus produces a quadrupole echo at $t=2\tau$ which achieves maximum amplitude when the second pulse rotation angle is about 55°. A similar calculation[8] for a $90°$-τ-$\beta_{90°}$ sequence yields

$$S(t)=(9/8)\sin^2\beta\int_{-\infty}^{\infty} f(a)[\cos 2a(t-2\tau)]da + \tfrac{1}{4}(1+3\cos^2\beta). \quad (3)$$

In the case of the $90°$-τ-$\beta_{90°}$ sequence, the echo achieves maximum amplitude when $\beta=90°$ and the echo amplitude is about $2\frac{1}{2}$ times greater than that of the $90°$-τ-$55°_{0°}$ echo. This suggests the advantage of using the $90°$-τ-$90°_{90°}$ sequence for study of gradient distributions under conditions of low signal-to-noise ratio.

Xenon crystallizes in the face-centered cubic structure and is ideally suited for experimental tests of the above ideas. Natural xenon contains two magnetic species: Xe^{129} (26.24% abundant) with $I=\frac{1}{2}$; and Xe^{131} (21.24% abundant) with $I=\frac{3}{2}$ and $Q=-0.12\times10^{-24}$ cm^2.[10] The low abundances, weak magnetic moments, and large interatomic distances lead to narrow dipolar broadened lines or, equivalently, long "dipolar" free-induction decays. One can therefore compare the free-induction decay and solid echo shapes with only modest requirements on the apparatus blocking time. Furthermore, a study of the effect of atomic diffusion on the dipolar interactions of Xe^{129} in solid xenon has been reported.[11] The correlation times for self-diffusion obtained in the Xe^{129} experiments are thus available for interpreting the effects of diffusion on the dipolar and quadrupolar interactions of Xe^{131}.

II. EXPERIMENTAL PROCEDURES

The 3.0 Mc/sec coherent pulsed nmr apparatus used to observe transient Xe^{129} and Xe^{131} signals has been described previously.[8,12] In the present experiments signals obtained at 4.2°K were demodulated by a diode without prior insertion of a reference signal at the resonance frequency, e.g., without utilizing coherent (phase-sensitive) detection.[13] The long spin-lattice relaxation time of either species at 4.2°K rendered it difficult to maintain the magnetic field at exact resonance between observations. This offset the advantages of coherent detection, since slight departures from resonance appeared as distortions of the long "dipolar" free-induction decay. Signals observed with simple diode detection were less sensitive to small changes of the magnetic field. For sequences in which the pulse spacing was of the order of the duration of the dipolar free-induction decay, the correct phase relationship between pulses was preserved by manually maintaining the field on resonance with a steady-state proton resonance obtained with a crystal-controlled marginal oscillator.[14] At higher temperatures, the short quadrupolar spin-lattice relaxation time[12] of Xe^{131} permitted convenient utilization of coherent detection for measurement of Xe^{131} spin-spin relaxation times.

The 90° phase shifts required for some sequences were obtained by the method of Meiboom and Gill.[15] Pulse widths for 180° pulses were adjusted by minimizing the free-induction decay following the pulse. The widths of the 90° pulses were then determined by adjust-

[10] Varian Associates (unpublished).
[11] W. M. Yen and R. E. Norberg, Phys. Rev. **131**, 269 (1963).
[12] W. W. Warren and R. E. Norberg, Phys. Rev. **148**, 402 (1966).
[13] J. J. Spokas and C. P. Slichter, Phys. Rev. **113**, 1462 (1959).
[14] R. L. Garwin, A. M. Patlach, and H. A. Reich, Rev. Sci. Instr. **30**, 79 (1959).
[15] S. Meiboom and D. Gill, Rev. Sci. Instr. **29**, 688 (1958).

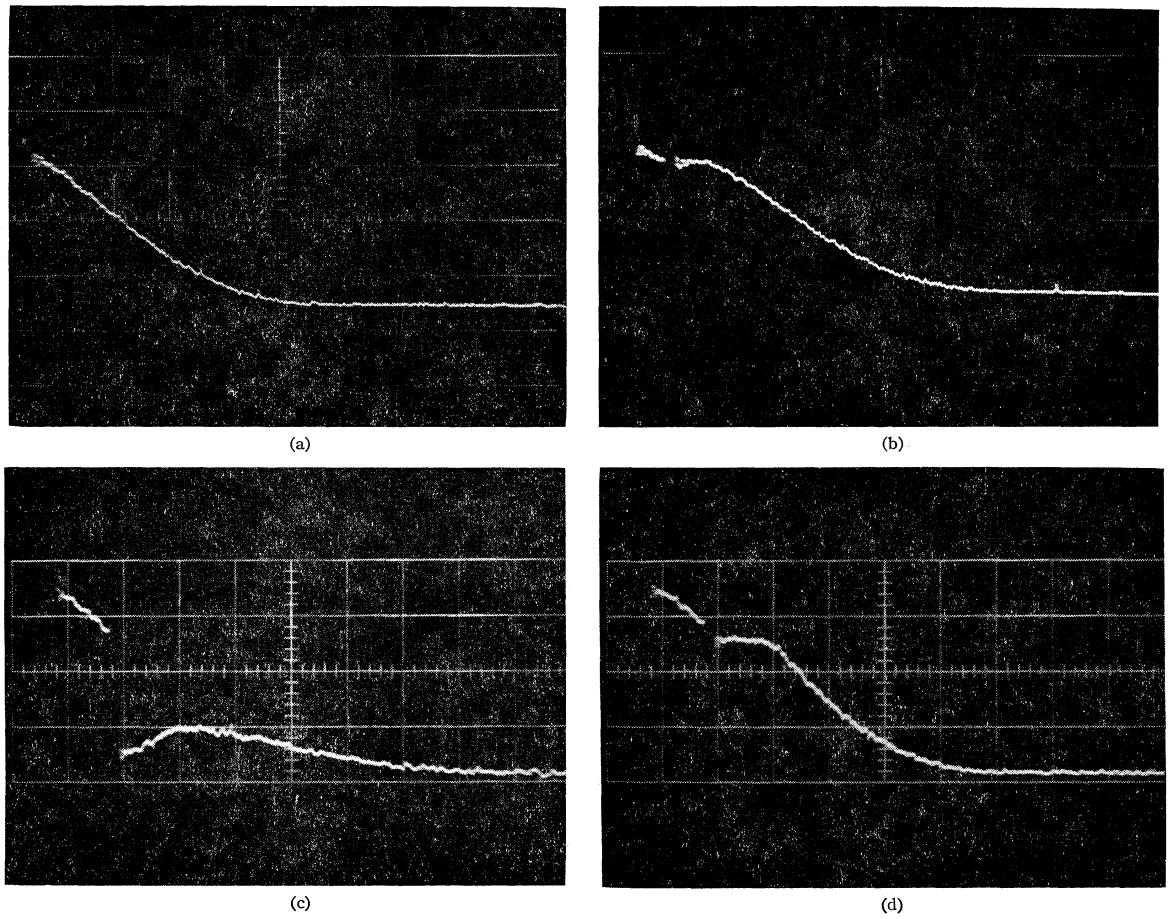

FIG. 1. Photographs of Xe^{129} transient signals in solid xenon at 4.2°K. The full length of each trace is 5 msec. (a) Free-induction decay following a 90° pulse. (b) Solid echo following a 90°-τ-90°$_{90}$° sequence with $\tau=0.40$ msec. (c) Transient signal following a 90°-τ-90°$_0$° sequence with $\tau=0.63$ msec. (d) Solid echo following a 90°-τ-180°$_0$° sequence with $\tau=0.63$ msec.

ing the pulse width to be half that of the 180° pulse or by minimizing the signal immediately following the second pulse of a 90°-τ-90°$_0$° sequence.

Xe^{131} spin-spin relaxation times T_2 were measured in the region of motional narrowing with Carr-Purcell-Meiboom[7,15] (CPM) and 90°-τ-180°$_0$° two-pulse sequences. Since the value of T_2 in the region of incipent motional narrowing was of the order of the dephasing time in the external field inhomogeneity, the homogeneity was deliberately degraded to improve the resolution of the echoes. Numerical values of T_2 were obtained graphically from semilogarithmic plots of the two-pulse and CPM echo envelopes.

The cryogenic techniques used for NMR studies of solid xenon have been described elsewhere.[8,12,16] For measurements of Xe^{131} spin-spin relaxation times at temperatures above the liquid-nitrogen bath temperature, heat was supplied by a bifilar manganin coil wound on a copper can enclosing the nylon sample holder. The heater can was removed for experiments at 4.2°K in order to eliminate ringing effects resulting from interaction between the copper can and the rf pulse. In the liquid-nitrogen temperature range such effects were negligible, and the copper can served to reduce thermal gradients in the sample container.

[16] W. M. Yen, thesis, Washington University, 1962 (unpublished).

III. EXPERIMENTAL OBSERVATIONS

A. Rigid Lattice: Xe^{129}

Xe^{129} free precession signals were observed in solid xenon at 4.2°K in a field of 2550 G. The samples were doped with small amounts of air (containing paramagnetic oxygen) which shortened the spin-lattice relaxation time to a convenient value—typically about 5 min. In the range of concentrations used, the free precession signal shapes were independent of impurity concentration.

1. Free-Induction Decay

The oscilloscope trace of a Xe^{129} free-induction decay is shown in Fig. 1(a). Yen and Norberg[11] studied the Xe^{129} decay at a field of 8920 G and showed the decay

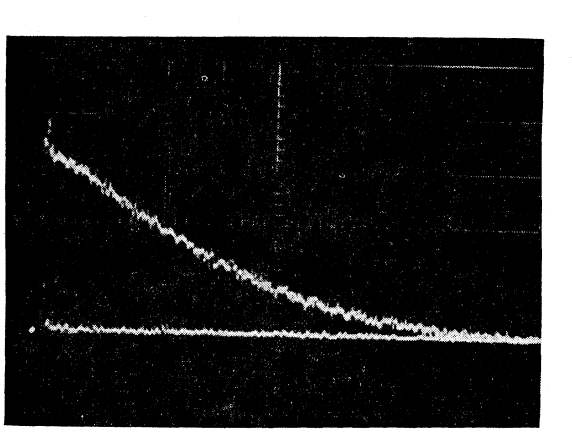

(a)

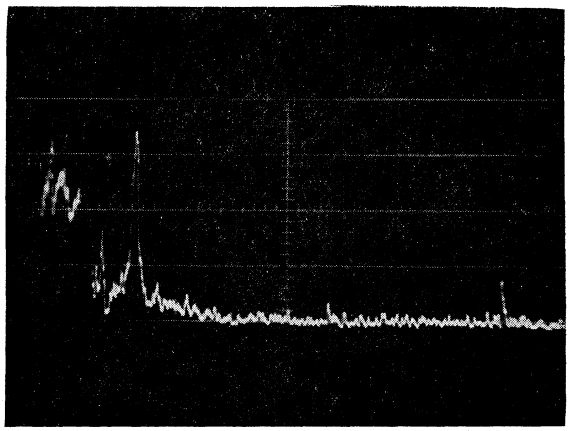

(b)

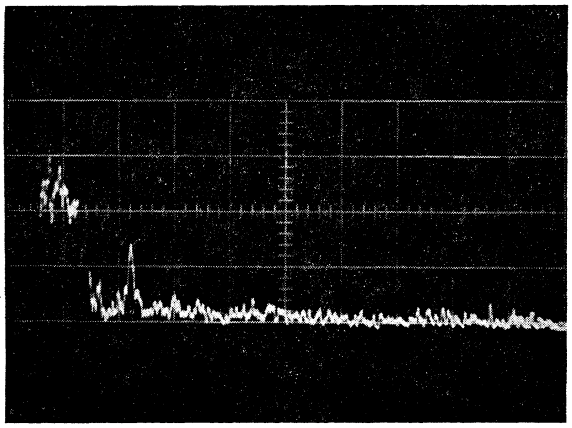

(c)

FIG. 2. Photographs of Xe^{131} transient signals in solid xenon at 4.2°K. (a) Free-induction decay following a 90° pulse. The full length of the trace is 10 msec. (b) Quadrupole echo following a 90°-τ-90°$_{90°}$ sequence with $\tau=0.50$ msec. The full length of the trace is 5 msec. (c) Quadrupole echo following a 90°-τ-55°$_{0°}$ sequence with $\tau=0.50$ msec. The full length of the trace is 5 msec.

shape to be very nearly Gaussian with a second moment, in substantial agreement with the Van Vleck theory of dipolar broadening in a rigid lattice.[17] In extracting the second moment from the observed free-induction decays, it was necessary to apply relatively large corrections to account for the dephasing effect of inhomogeneity in the external field. At the lower value of the external field used in the present experiments, the effect of inhomogeneity was negligible and the observed free-induction decay shape was assumed to be determined solely by the dipole-dipole interactions.

The free-induction decay shown in Fig. 1(a) was analyzed by assuming a Gaussian decay of the form

$$S(t)=S(0)\ \exp(-t^2/2T_{2G}^2), \qquad (4)$$

with $T_{2G}=0.97\pm0.03$ msec. This yields the second moment $\sigma^2=T_{2G}^{-2}=1.06\pm0.08\times10^6$ sec^{-2} (free-induction decay). Second moments were computed by the method of Van Vleck[17] for polycrystalline natural xenon at 4.2°K. The results are

$$\sigma_{129\text{-}129}{}^2=0.85\times10^6\ \text{sec}^{-2},$$
$$\sigma_{129\text{-}131}{}^2=0.13\times10^6\ \text{sec}^{-2}.$$

These yield the total second moment

$$\sigma^2=0.98\times10^6\ \text{sec}^{-2}\quad\text{(theory)}.$$

The observed free-induction decay is therefore in agreement with the theoretical dipolar second moment and with the results of Yen and Norberg.

2. 90°-τ-90°$_{90°}$ *Solid Echo*

Figure 1(b) shows the signal obtained when a second 90° pulse is phase-shifted by 90° relative to the initial 90° pulse and applied at $t=\tau$. The result is the predicted solid echo[4] at $t=2\tau$. The difference between the amplitude of the signal at $t=2\tau$ and the initial amplitude $S(0)$ is a measure of the irreversibility of the spin-spin relaxation process. The time dependence of the signal beginning at $t=2\tau$ was analyzed and found to be Gaussian with the form

$$S_e(t)=S_e(2\tau)\ \exp[-(t-2\tau)^2/2T_{2G}^2], \qquad (5)$$

where $T_{2G}=1.00\pm0.03$ msec. The solid echo shape therefore reproduces the shape of the free-induction decay to within experimental error. This observation supports the suggestion of Mansfield[4] that the 90°-τ-

[17] J. H. Van Vleck, Phys. Rev. 74, 1168 (1948).

$90°_{90°}$ sequence should be useful for determining the shape of the free-induction decay in cases in which the initial portion of the decay is obscured by blocking of the apparatus.

3. $90°$-τ-$90°_{0°}$ Transient

Mansfield[4] has shown that the signal following application of a $90°$-τ-$90°_{0°}$ sequence to a system containing two magnetic species has the general character of a derivative free-induction decay characterized by the nonresonant second moment contribution σ_{IS}^2. The expected signal is given by an expansion of the form

$$S(t)=-S(0)\left[\sigma_{IS}{}^2\tau(t-2\tau)+M_{41}{}^{IS}\frac{\tau^3(t-2\tau)}{3!}+M_{42}{}^{IS}\frac{\tau^2(t-2\tau)^2}{4}+M_{43}{}^{IS}\frac{\tau(t-2\tau)^3}{3!}+\cdots\right]. \quad (6)$$

The coefficients $M_{41}{}^{IS}$, $M_{42}{}^{IS}$, $M_{43}{}^{IS}$ are related to the fourth-moment contribution of the nonresonant species and $S(0)$ is the initial amplitude of the free-induction decay. Mansfield has described a method of determining σ_{IS}^2 by analyzing the dependence of the initial slope $S'(\tau)$ on the pulse spacing τ.

The Xe^{129} signal obtained with a $90°$-τ-$90°_{0°}$ sequence is shown in Fig. 1(c). The modulus of the signal occurring after the second $90°$ pulse exhibits the general features predicted by Eq. (6). Unfortunately, the initial slope of this signal was found to be extremely sensitive to the $90°$ pulse width and to tuning of the magnetic field. This difficulty led to large variations in the values of σ_{IS}^2 determined by Mansfield's method and the data yielded only an order of magnitude measurement.

4. $90°$-τ-$180°_{0°\text{ or }90°}$ Solid Echo

The Hamiltonian describing the dipolar interaction of the resonant species I with the nonresonant species S is

$$\mathcal{H}_{IS}=\sum_{i,\alpha} C_{i\alpha}I_z{}^iS_z{}^\alpha \quad (7)$$

with

$$C_{i\alpha}=(\gamma_I\gamma_S\hbar^2/r_{i\alpha}{}^3)(1-3\cos^2\theta_{i\alpha}).$$

With respect to operations on the resonant species I, the Hamiltonian (7) has the same rotational symmetry properties as the term of the Zeeman Hamiltonian describing the effect of an inhomogeneous magnetic field:

$$\mathcal{H}_{\Delta H}=\gamma_I\hbar\sum_i I_z{}^i\Delta H_i, \quad (8)$$

where ΔH_i is the difference between the field at the site of the ith nucleus and the average applied field H_0. In a two-species system, therefore, one is led to expect $90°$-τ-$180°_{90°}$ sequence or a $90°$-τ-$180°_{0°}$ sequence to lead to formation of an echo analogous to the "conventional" spin echo[6,7] obtained in an inhomogeneous magnetic field. In a rigid solid, application of a $180°$ pulse inverts the I spins relative to the local fields produced by the S spins. It is easily shown[8] that to zeroth order in the commutator $[\mathcal{H}_{II}+\mathcal{H}_{SS},\mathcal{H}_{IS}]$, an echo is formed at $t=2\tau$ with maximum amplitude equal to the amplitude at $t=2\tau$ of a free-induction decay in which the only broadening interaction present is the resonant spin dipolar interaction $\mathcal{H}_{II}$. By observing $90°$-τ-$180°$ echoes with various values of τ, it should therefore be possible to make a direct determination of σ_{II}^2, the resonant spin contribution to the second moment in a two species system.

The Xe^{129} solid echo obtained with a $90°$-τ-$180°_{0°}$ sequence is shown in Fig. 1(d). The envelope of the signal amplitude at $t=2\tau$ was found to be nearly Gaussian with $T_{2G}=1.5\pm0.1$ msec. This yields for the resonant spin contribution

$$\sigma_{129\text{-}129}{}^2=0.44\pm0.06\times10^6\ \text{sec}^{-2}\quad\text{(solid echo)}.$$

This value is approximately one-half that expected from the Van Vleck theory. Since the resonant spin (Xe^{129}—Xe^{129}) interaction makes the major contribution to the total second moment and since the experimental second moments determined from the free-induction decay are in good agreement with theory, it is clear that the echo amplitudes for large τ differ appreciably from the zeroth-order prediction of theory.

B. Rigid Lattice: Xe^{131} ($I=\frac{3}{2}$)

Xe^{131} free precession signals were observed in solid xenon at 4.2°K in a field of 8600 G. The samples used for Xe^{131} studies were the same as those used for the Xe^{129} measurements. The Xe^{131} spin-lattice relaxation time at 4.2°K was typically about 10 min.

1. Free-Induction Decay

The oscilloscope trace of a typical Xe^{131} free-induction decay is shown in Fig. 2(a). Analysis of the shape of the decay was complicated by the fact that over the duration of the free-induction decay, dephasing due to inhomogeneity of the magnetic field was not negligible. A correction was made by assuming the observed signal to have the form

$$S(t)=S_d(t)S_m(t), \quad (9)$$

where $S_d(t)$ is the true free-induction-decay shape and $S_m(t)$ is a function determined by the magnet inhomogeneity. The function $S_m(t)$ was obtained from free-induction-decay shapes observed in liquid xenon. The logarithm of the corrected free-induction signal amplitude is plotted against t^2 in Fig. 3. Although the curvature of the data indicates that the decay is not Gaussian, a Gaussian analysis is useful to obtain an approximate parameter to characterize the decay time. The solid line in Fig. 3 represents roughly the average slope of the Xe^{131} data and yields a value for a Gaussian spin-spin relaxation time $T_{2G}\approx3.6$ msec.

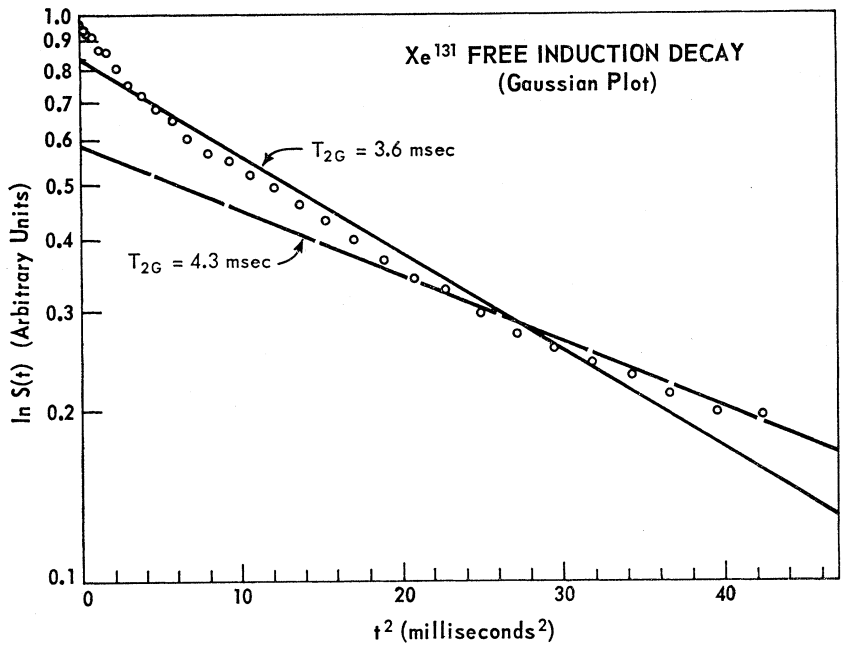

FIG. 3. Semilogarithmic analysis of Xe^{131} free-induction decay. The solid line approximately represents the average slope of the data. The broken line corresponds to a Gaussian decay characterized by the theoretical second moment.

The observation of quadrupole echoes[2] in solid xenon and intensity loss in the Xe^{131} free-induction decay at the transition from liquid to solid indicates that the free-induction decay observed in the solid corresponds to only the central ($m=\pm\frac{1}{2}$) transition, e.g., the "*time-independent*" part of Eq. (1). Moreover, the signal amplitude in the solid just below the melting point was approximately $\frac{2}{5}$ of the amplitude in the liquid, in good agreement with Eq. (1). The "*quadrupolar*" component of the free-induction decay occurs during the blocking time of the apparatus.

The theory of dipolar broadening of the central component of a first-order quadrupolar broadened line has been given by Kambe and Ollom.[18] For the case of Xe^{131} nuclei in a solid xenon sample in which the electric field gradient varies from site to site, the theory predicts for the resonant spin contribution to the central linewidth

$$\sigma_{131\text{-}131}{}^2=0.021\times10^6 \text{ sec}^{-2}.$$

Evaluation of the Van Vleck expression[17] for the nonresonant contribution to the second moment yields

$$\sigma_{131\text{-}129}{}^2=0.032\times10^6 \text{ sec}^{-2}.$$

The total second moment is then

$$\sigma^2=0.053\times10^6 \text{ sec}^{-2} \quad \text{(theory)}.$$

The slope of the broken line in Fig. 3 corresponds to this value for the theoretical second moment. The total second moment derived from the approximate Gaussian analysis of the free-induction decay is

$$\sigma^2=T_{2G}{}^{-2}=0.077\times10^6 \text{ sec}^{-2} \quad \text{(free-induction decay)}.$$

[18] K. Kambe and J. K. Ollom, J. Phys. Soc. Japan **11**, 50 (1956).

In the contrast to the case of Xe^{129}, the Xe^{131} free-induction decay is (1) non-Gaussian and (2) of somewhat shorter duration than one expects if only dipolar broadening of the central transition is considered. This suggests the presence of second-order quadrupole interactions in the polycrystalline samples. Measurements of the strength of the quadrupole interaction by means of quadrupole echoes confirmed in fact, that second-order effects were of the same order of magnitude as the dipolar interactions.

Abragam[19] has suggested an additional mechanism which may contribute to the non-Gaussian character of the free-induction decay. In a system containing two species of approximately equal abundance, the various terms in the expression for the fourth moment M_4 are approximately proportional to $\gamma_I{}^8$, $\gamma_I{}^6\gamma_S{}^2$, $\gamma_I{}^4\gamma_S{}^4$, and $\gamma_I{}^2\gamma_S{}^6$. In the case of Xe^{131}, $\gamma_S/\gamma_I\approx3.5$ so that the $\gamma_I{}^2\gamma_S{}^6$ term dominates the fourth moment. Then

$$M_4/\sigma^4\propto(\gamma_S/\gamma_I)^2\approx10,$$

whereas in the ideal Gaussian case, $M_4/\sigma^4=3$. The rapid mutual "flip-flops" among the nonresonant spins thus lead to a kind of "motional narrowing" of the nonresonant contribution and a quasi-Lorentzian line shape. This is consistent with analysis of the Xe^{131} decay shape which showed the decay to be intermediate between a Gaussian and an exponential.

2. *90°-τ-55°₀° and 90°-τ-90°₉₀° Quadrupole Echoes*

Xe^{131} quadrupole echoes obtained with 90°-τ-55°₀° and 90°-τ-90°₉₀° sequences are shown in Figs. 2(c) and

[19] A. Abragam, *The Principles of Nuclear Magnetism* (Clarendon Press, Oxford, England, 1961), Chap. IV.

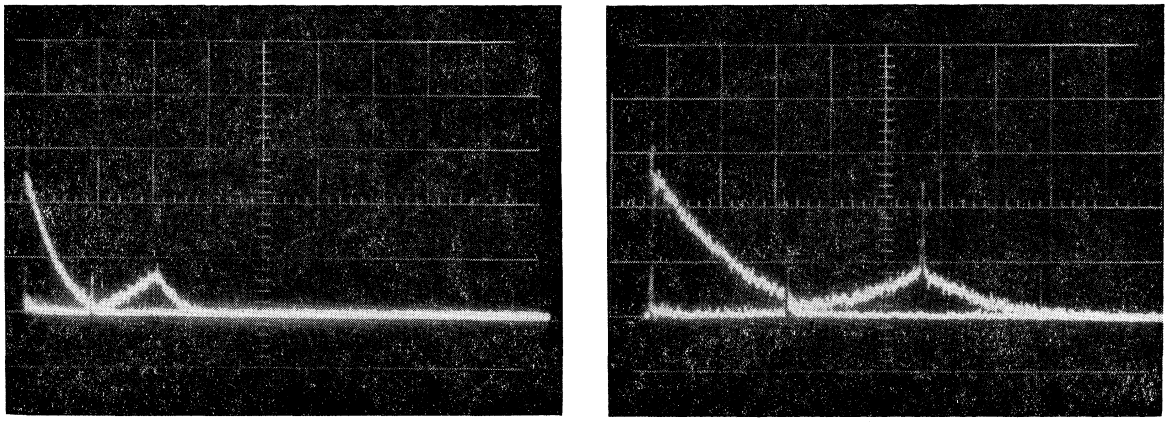

(a) (b)

FIG. 4. Photographs of Xe^{131} transient signals in solid xenon at 4.2°K. (a) Solid echo following a $90°$-τ-$180°_0°$ sequence with $\tau=6.3$ msec. The full length of the trace is 50 msec. (b) Compound solid-quadrupole echo following a $90°$-τ-$55°_0°$ sequence with $\tau=4$ msec. The full length of the trace is 20 msec.

2(b), respectively. The prediction of Eqs. (2) and (3) for a larger quadrupole echo with the $90°$-τ-$90°_{90°}$ sequence is clearly borne out. The dependence of the $90°$-τ-$\beta_{90°}$ echo amplitude on the second pulse width β was investigated[8] and found to be in qualitative agreement with Eq. (3).

Solomon[2] has shown that if the rotating rf field H_1 is of insufficient magnitude, the echo shape is not given rigorously by Eqs. (2) and (3). For small H_1 fields, the echo width should be proportional to H_1 since in that case the pulse only rotates those spins for which $|a| \lesssim \gamma H_1$. On the other hand, if $\langle a^2\rangle^{1/2} \ll \gamma H_1$, the echo shape should reproduce the true shape of the gradient distribution $f(a)$.

In the present experiments, maximum H_1 was about 22 G. Investigation of the H_1 dependence of the echo width showed that $T_{1/2}$, the echo full width at half-maximum was dependent on H_1 although $dT_{1/2}/dH_1$ was sufficiently small at $H_1=22$ G to permit an estimate of the width of the gradient distribution in a typical polycrystalline xenon sample:

$$\frac{1}{4\pi T_{1/2}}=\frac{3eQ\langle V_{zz}^2\rangle^{1/2}}{4I(2I-1)h}=2.4\pm0.2 \text{ kc}.$$

It is possible to use the above result to estimate the relative magnitude of the second-order quadrupole effect. Second-order shifts of the nuclear Zeeman levels are of the order of $4\langle a^2\rangle/\omega_0$[20] and the ratio of the second-order shift to the dipolar root second moment is

$$4\langle a^2\rangle/\omega_0\sigma\approx 0.2.$$

It is clear that second-order quadrupole broadening of the central line is not negligible. The effect is, in fact, of sufficient magnitude that it could be responsible for the lack of agreement between the observed "dipolar" free-induction decay and the Van Vleck theory of dipolar broadening.

Cohen and Reif[20] have shown that a Gaussian gradient distribution results from a large concentration of defects, whereas low concentrations produce Lorentzian distributions. Analysis of the shape of the Xe^{131} quadrupole echo showed it to be very nearly Gaussian, indicating that the density of defects in these samples was large enough that each nucleus was affected by several sources of electric field gradient. Possible sources of the electric field gradients include impurities, dislocations, and surface effects in the polycrystalline samples. The echo widths were reproducible to within $\pm 10\%$ in samples solidified on different occasions and with differing impurity concentrations. Observation of the echoes in samples with low-impurity concentrations indicated that the gradient distribution did not result from the presence of a hexagonal phase of the kind reported for solid argon-nitrogen mixtures.[21,22] Attempts to reduce the average field gradient by annealing dislocations at temperatures about 10°K below the melting point were not successful.

3. Xe^{131} Solid ("Dipolar") Echoes

The solid echo obtained with a $90°$-τ-$180°_0°$ sequence applied to Xe^{131} at 4.2°K is shown in Fig. 4(a). The echo is presumably of the same type as the echo obtained with the same sequence applied to Xe^{129} [Fig. 1(d)]. The Xe^{131} echo is more clearly defined than the Xe^{129} echo since in the case of Xe^{131}, dipolar interactions with the nonresonant species make the major contribution to the total second moment. Moreover, for Xe^{131} there is a small contribution to the echo amplitude due to rephasing of the spins in the external magnetic field gradient.

[20] M. H. Cohen and F. Reif, in *Solid State Physics*, edited by F. Seitz and D. Turnbull (Academic Press Inc., New York, 1957), Vol. 5.

[21] L. Meyer, C. S. Barrett, and P. Haasen, J. Chem. Phys. **40**, 2744 (1964).

[22] C. S. Barrett and L. Meyer, J. Chem. Phys. **42**, 107 (1965).

The envelope of the Xe^{131} 90°-τ-180°$_0$° echo amplitude was found to be approximately Gaussian with $T_{2G}=9.5\pm0.5$ msec. This yields the following value for the resonant spin contribution to the second moment:

$$\sigma_{131\text{-}131}{}^2=0.011\pm0.001\times10^6 \text{ sec}^{-2} \quad \text{(solid echo)}.$$

By comparison, the theoretical prediction is

$$\sigma_{131\text{-}131}{}^2=0.021\times10^6 \text{ sec}^{-2} \quad \text{(theory)}.$$

This discrepancy between the theoretical value of $\sigma_{II}{}^2$ and the envelope of the 90°-τ-180°$_0$° echo is similar to the discrepancy found in the analogous case for Xe^{129}. It seems clear that the simple interpretation of the 90°-τ-180°$_0$° echo formation given in Sec. IIIA, while qualitatively correct, is not adequate to permit an accurate measurement of $\sigma_{II}{}^2$ and that terms involving the commutator $[\mathcal{H}_{II}+\mathcal{H}_{SS}, \mathcal{H}_{IS}]$ should be taken into account.

It is difficult to interpret the effect of 90°-τ-90°$_{90}$° and 90°-τ-90°$_0$° sequences on the dipolar part of the Xe^{131} signal due to the presence of quadrupolar broadening produced by defects in the solid xenon samples. Although Mansfield[4] has calculated the response for multiple-pulse sequences applied to the central component of a *well-resolved* quadrupole split line, the present case, namely the dipolar broadened central component in an imperfect cubic crystal, has not yet been treated. In the absence of a quadrupole interaction, we would expect only a weak Xe^{131} dipolar solid echo following a 90°-τ-90°$_{90}$° sequence since the theory indicates that no solid echo should occur if $\sigma_{IS}{}^2\gg\sigma_{II}{}^2$. In the case of Xe^{131} the calculated second moment contributions give $\sigma_{131\text{-}129}{}^2/\sigma_{131\text{-}131}{}^2=1.6$ and, in fact, relatively little rephasing of the dipolar portion of the signal was observed after a 90°-τ-90°$_{90}$° sequence. In contrast, for Xe^{129} $\sigma_{129\text{-}131}{}^2/\sigma_{129\text{-}129}{}^2=0.15$ and an echo could be obtained [Fig. 1(b)].

Finally, we present in Fig. 4(b) a compound echo obtained with a 90°-τ-55°$_0$° sequence for which the pulse spacing τ was of the order of the duration of the "dipolar" free-induction decay. The time dependence of the slowly varying part of the echo is similar to that of the dipolar signal, while the sharp spike at $t=2\tau$ is nearly identical to the quadrupole echo obtained with short pulse spacings. The slowly varying part of the signal may be related to the transient predicted by Mansfield for a 90°-τ-90°$_0$° sequence. There clearly exists the need for an extension of the theory to systems containing two magnetic species and exhibiting quadrupole broadening from random defects in a cubic crystal.

C. Effect of Atomic Motion on Free-Precession Signals: Xe^{131}

The free-induction decays and multiple-pulse transients described in the preceding sections are characteristic of solid xenon samples in which thermal atomic motions are slow compared to the duration of the free-precession signals. However, as the temperature of the sample is raised, one expects atomic motion to have important effects on the dipolar and quadrupolar interactions.[23,24] In particular, one expects motional narrowing of the dipolar and quadrupolar broadened parts of the resonance line when the correlation time τ_c for atomic diffusion is shorter than the duration of the corresponding free induction decays in the rigid solid.

1. Motional Narrowing of the Central ($m=\pm\frac{1}{2}$) Transition

Kubo and Tomita[25] have applied the methods of irreversible quantum-statistical mechanics to the problem of dipolar broadening in the presence of atomic motion; they have shown that for $\tau_c\sigma<1$, in the adiabatic limit ($\omega_0\tau_c\gg1$) the absorption line should be Lorentzian with a half-width at half-maximum $\Delta\omega=1/T_{2L}$ where

$$\left(\frac{1}{T_{2L}}\right)^2=\frac{4\ln2}{\pi}\sigma^2\tan^{-1}\left(\frac{\pi\tau_c}{(4\ln2)T_{2L}}\right). \tag{10}$$

For a Gaussian line in the rigid lattice ($\tau_c\sigma\gg1$), Eq. (10) reduces to

$$1/T_{2G}=\sigma$$

while for the well narrowed line

$$1/T_{2L}=\sigma^2\tau_c.$$

It has been shown[26] that for diffusion in a fcc lattice,

$$\tau_c=d^2/12D, \tag{11}$$

where d is the cube edge parameter and D is the coefficient of self-diffusion. Thus, measurements of T_{2L} and σ combined with knowledge of d permit determination of the diffusion coefficient D. If the temperature dependence of D is described by an Arrhenius relation

$$D=D_0\exp(-E_D/RT), \tag{12}$$

the inverse linewidth T_{2L} should increase exponentially with increasing temperature.

In situations where the motionally narrowed linewidth is less than the average inhomogeneity in the magnetic field over the sample volume, the inverse linewidth or spin-spin relaxation time T_{2L} can be measured by means of 90°-τ-180° (two-pulse) spin echoes or Carr-Purcell-Meiboom (CPM) sequences.[7,15] Using these techniques, Yen and Norberg[11] investigated motional narrowing of the Xe^{129} resonance in solid xenon and found that T_{2L} increases by three orders of magnitude between 115 and 160°K. These authors were

[23] N. Bloembergen, E. M. Purcell, and R. V. Pound, Phys. Rev. 73, 679 (1948).
[24] W. G. Clark, thesis, Cornell University, 1961 (unpublished).
[25] R. Kubo and K. Tomita, J. Phys. Soc. Japan 9, 888 (1954).
[26] H. C. Torrey, Phys. Rev. 92, 962 (1953).

able to extract the activation energy for self-diffusion E_D, the diffusion constant D_0 and the correlation time τ_c from the T_{2L} data.

Since their masses differ by less than 2%, Xe^{129} and Xe^{131} should diffuse with nearly the same coefficient of self-diffusion. The correlation times obtained from Xe^{129} studies may therefore be used to predict the effects of atomic motion on the Xe^{131} dipolar linewidth. Motional narrowing should commence at a temperature such that $\tau_c \approx \sigma^{-1}$.[23] The theoretical value of σ indicates that this temperature is 119°K for Xe^{131}. Above this temperature T_{2L} should increase exponentially, governed by essentially the same activation energy E_D as Xe^{129}. Measurement of T_{2L} for Xe^{131} in the motionally narrowed temperature range should therefore provide a useful independent check on the Xe^{129} diffusion measurements.

Spin-spin relaxation data for Xe^{131} are presented in Fig. 5 together with T_1 data for the solid and liquid above 90°K. T_2 was measured from the rigid lattice to 175°K with 90°-τ-180°$_0$° and CPM sequences. Data obtained above 110°K were analyzed by assuming exponential echo envelopes (Lorentzian line shape),

$$S_e(t) \propto \exp(-t/T_{2L}),$$

while below this temperature a Gaussian envelope was assumed,

$$S_e(t) \propto \exp(-t^2/2T_{2G}^2).$$

It is interesting to note that as a result of the presence of two magnetic species and the formation of 90°-τ-180° solid echoes of the type shown in Figs. 1(d) and 4(a), the echo envelope remains greater than $T_{2G}=(\sigma_{131\text{-}131})^{-1}$ in the rigid lattice. The same qualitative behavior was exhibited by 90°-τ-180° echo envelopes at 4.2°K. Because of poor signal-to-noise ratio and ambiguity introduced by the necessary corrections for magnetic-field inhomogeneity, analysis of free-induction decays in the region of incipient motional narrowing was not attempted.

The steep broken line in Fig. 5 is drawn with a slope corresponding to the activation energy for self-diffusion obtained by Yen and Norberg[11] and intersects $T_{2G}=\sigma^{-1}$ at the temperature for which $\sigma\tau_c=1$. The onset of motional narrowing clearly occurs where expected on the basis of Yen and Norberg's results. The initial slope of the Xe^{131} data is very nearly the same as that of the Xe^{129} data while at higher temperatures, T_{2L} deviates from the expected dipolar behavior under the influence of strong quadrupolar T_1 processes. At temperatures near the melting point, the T_{2L} data show a broad maximum and T_{2L} approaches T_1. Lifetime broadening thus limited the measurement of the Xe^{131} dipolar T_{2L} to a relatively small temperature range, and it was not possible to extract a meaningful activation energy from the data.

A sharp decrease in both T_1 and T_2 is evident at the melting point. The shorter spin-lattice relaxation times in the liquid are due to the much higher frequency of

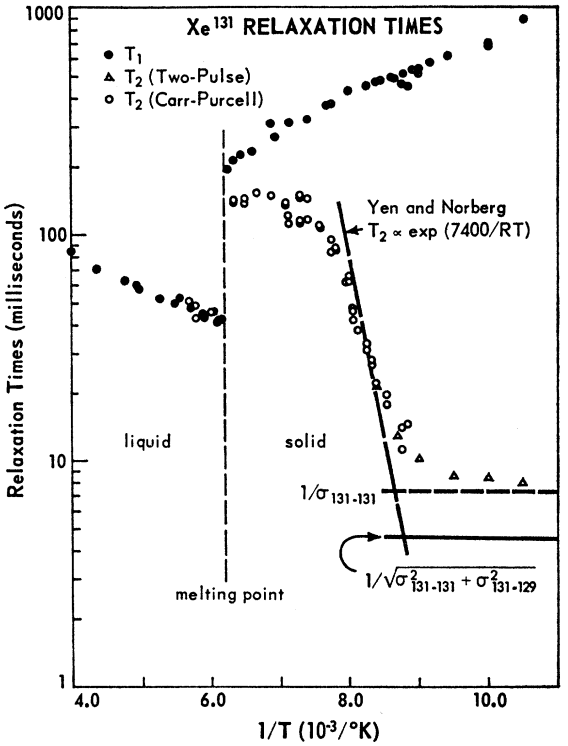

FIG. 5. Spin-spin and spin-lattice relaxation times for Xe^{131} in solid and liquid xenon. The broken line is drawn with a slope corresponding to the activation energy for self-diffusion reported in Ref. 11; it intersects the rigid lattice Gaussian T_{2G} (solid line) at the temperature for which $\tau_c=T_{2G}$. The T_1 data are quoted from Ref. 12. Note that T_{2G} values obtained from the envelopes of 90°-τ-180°$_0$° solid echoes remain greater than $T_{2G}=1/\sigma_{131\text{-}131}$ in the rigid lattice.

atomic motion in that phase. The Xe^{129} correlation times obtained by Yen and Norberg[11] indicate that for Xe^{131} in liquid xenon at a resonance frequency of 3.0 Mc/sec,

$$\omega_0\tau_c \approx 10^{-4} \ll 1.$$

Therefore, the conditions of "extreme narrowing"[27] should hold in the liquid. The equality of T_1 and T_2 for Xe^{131} in liquid xenon is good evidence that this is actually the case.

2. *Effect of Atomic Motion on the Quadrupolar Interaction*

As diffusion increases, the internal electric field gradients which are responsible for the quadrupole free-induction decay and quadrupole echo also become time-dependent. A diffusing atom samples various electric field gradients within the distribution $f(a)$ so that the average gradient experienced by a given nucleus decreases. By analogy with the case of dipolar broadening, the quadrupolar broadened portion of the line should begin to be affected when the correlation time for the quadrupolar interaction τ_q is roughly equal to the inverse width of the static broadening.

[27] A. Abragam, Ref. 19, Chap. X.

Multiple pulse experiments at 4.2°K indicate that $\langle a^2\rangle \gg \sigma^2$; thus, the quadrupolar broadened portion of the resonance ought to begin to exhibit the effects of atomic motion at a higher temperature than the dipolar broadened portion. After narrowing commences, the quadrupolar free-induction decay should lengthen with increasing temperature until both the dipolar and quadrupolar decays are lifetime limited by T_1 processes. A similar effect should occur for the quadrupole echo.[24]

The temperature at which the quadrupolar broadened portion of the line should be affected by atomic motion was estimated using the experimental Xe^{129} correlation times for self-diffusion and the measured width of the static broadening. The correlation time τ_q after which the quadrupole interaction changes appreciably ought to be somewhat longer than the mean time τ_c between diffusion jumps since several jumps may be required before the gradient changes. Given the high density of defects suggested by the Gaussian quadrupole echo shape,[20] a reasonable guess might be $\tau_q \approx 10\tau_c$. If this is assumed, we should expect that at the melting point, $\langle a^2\rangle \approx 10^7$ sec^{-2}; thus, the mean quadrupolar broadening would still be much greater than the width of the inhomogeneously broadened central line. On the other hand, in the liquid τ_c decreases by about five orders of magnitude[11] so that the effects of static quadrupolar broadening in the liquid should be negligible compared to quadrupolar lifetime broadening. The free-induction decay amplitude increased by a factor of approximately $\frac{5}{2}$ when the sample melted, indicating that quadrupolar broadening does indeed vanish in the liquid. The factor $\frac{5}{2}$ is in excellent agreement with Eq. (1) in the limit $f(a)\sim\delta(0)$.

Because of poor signal-to-noise ratio at temperatures near the melting point, it was not possible to observe the quadrupole echo and investigate the effect of diffusion on its shape and position.[24] Hence, the only statement that we can make concerning the effect of diffusion on Xe^{131} quadrupolar broadening is that motional narrowing probably commences in the solid near the melting point and that quadrupolar broadening is certainly absent in liquid xenon.

IV. SUMMARY

Xe^{129} and Xe^{131} multiple pulse transients observed in solid xenon at 4.2°K were consistent with the theories of Mansfield and Solomon. The decay of the Xe^{129} 90°-τ-90°$_{90°}$ solid echo reproduced the shape of the free-induction decay to within experimental error while, as expected from theory, a well-defined echo was not obtained from Xe^{131}. Although the Xe^{129} signal following a 90°-τ-90°$_{0°}$ sequence was in qualitative agreement with theory, it was not possible to obtain an accurate measurement of $\sigma_{129\text{-}131}{}^2$. In the case of Xe^{131}, interpretation of the 90°-τ-90°$_{0°}$ sequence was complicated by the presence of quadrupolar broadening and formation of quadrupole echoes. Well defined 90°-τ-180° solid echoes were obtained for both Xe^{129} and Xe^{131}. As the pulse spacing τ was increased, the echo amplitude decreased more slowly than the simple local-field model would suggest. The value of $\sigma_{II}{}^2$ for either species determined from the 90°-τ-180° solid echo envelope is roughly one-half the theoretical value.

Quadrupole echoes obtained from Xe^{131} at 4.2°K yielded an estimate of the typical strength of the quadrupole interaction due to random defects in the solid xenon samples. On the basis of this estimate, the Xe^{131} free-induction decay was interpreted as corresponding to the central ($m=\pm\frac{1}{2}$) component of the spectrum. The broadening of this component is mainly dipolar in origin with approximately a 20% contribution from second-order quadrupole interactions. Investigation of Xe^{131} quadrupole echoes verified that introduction of a 90° shift in the relative phases of the two pulses in a sequence leads to a quadrupole echo which attains maximum amplitude if the second pulse produces a 90° rotation (90°-τ-90°$_{90°}$ sequence).

Xe^{131} spin-spin relaxation times measured with "conventional" 90°-τ-180° spin echoes indicate that motional narrowing of the Xe^{131} central component occurs at the temperature expected from the correlation times for self-diffusion obtained by Yen and Norberg. Within the small temperature range between the onset of motional narrowing and the onset of lifetime broadening, the temperature dependence of the Xe^{131} T_2 data is in agreement with the activation energy for self-diffusion reported by Yen and Norberg.

ACKNOWLEDGMENTS

The authors are indebted to Professor K. Luszczynski for many helpful discussions. Professor W. G. Clark read the manuscript and offered several useful suggestions.

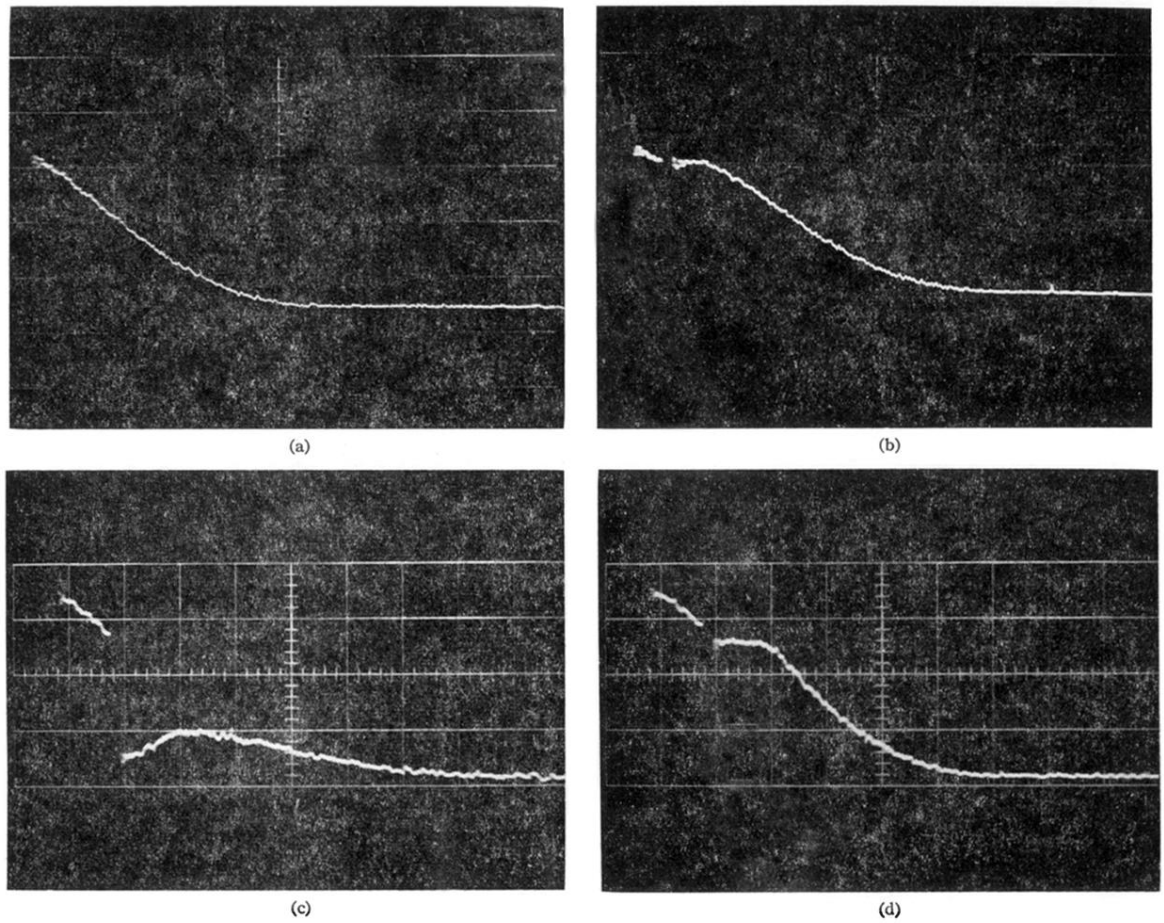

FIG. 1. Photographs of Xe^{129} transient signals in solid xenon at 4.2°K. The full length of each trace is 5 msec. (a) Free-induction decay following a 90° pulse. (b) Solid echo following a $90°\text{-}\tau\text{-}90°_{90°}$ sequence with $\tau=0.40$ msec. (c) Transient signal following a $90°\text{-}\tau\text{-}90°_{0°}$ sequence with $\tau=0.63$ msec. (d) Solid echo following a $90°\text{-}\tau\text{-}180°_{0°}$ sequence with $\tau=0.63$ msec.

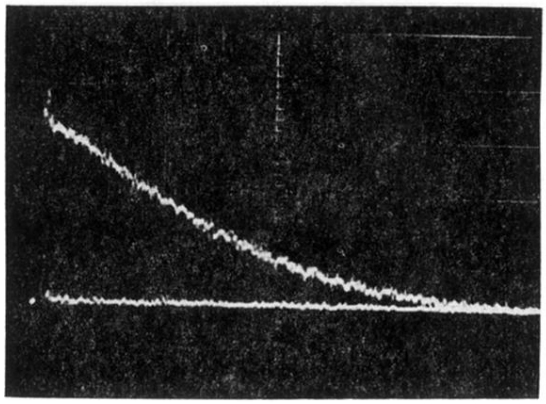

(a)

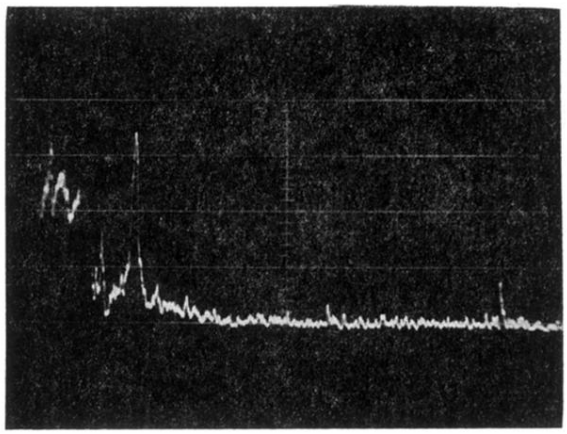

(b)

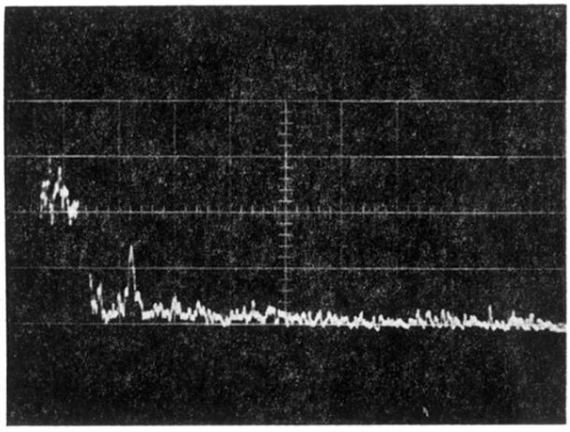

(c)

FIG. 2. Photographs of Xe^{131} transient signals in solid xenon at 4.2°K. (a) Free-induction decay following a 90° pulse. The full length of the trace is 10 msec. (b) Quadrupole echo following a $90°$-τ-$90°_{90°}$ sequence with $\tau=0.50$ msec. The full length of the trace is 5 msec. (c) Quadrupole echo following a $90°$-τ-$55°_{0°}$ sequence with $\tau=0.50$ msec. The full length of the trace is 5 msec.

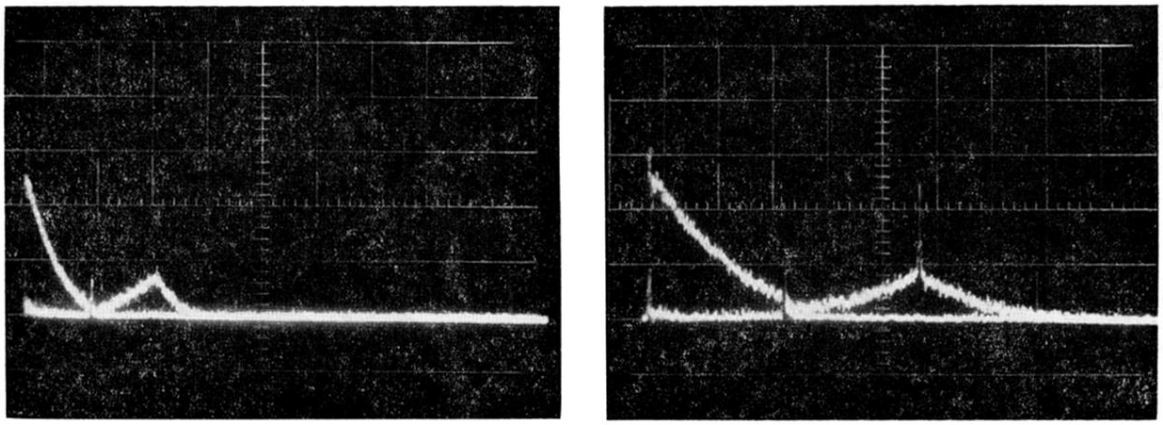

(a) (b)

FIG. 4. Photographs of Xe^{131} transient signals in solid xenon at 4.2°K. (a) Solid echo following a 90°-τ-180°$_0$° sequence with $\tau=6.3$ msec. The full length of the trace is 50 msec. (b) Compound solid-quadrupole echo following a 90°-τ-55°$_0$° sequence with $\tau=4$ msec. The full length of the trace is 20 msec.